Quark-mass effects for energy-energy correlations in high-energy e^-e^+ annihilation

F. Csikor
Institute for Theoretical Physics, Eötvös University, Budapest, Hungary
(Received 14 November 1983; revised manuscript received 28 February 1984)

Quark-mass effects for energy-energy correlations in high-energy e^-e^+ annihilation are calculated for arbitrary initial-state polarizations. While the contribution of the massive quark depends sensitively on the mass/(total center-of-mass energy) ratio, the normalized, angle-integrated correlation is much less sensitive to the quark mass. In particular, at the Z^0 peak, the normalized, angle-integrated energy-energy correlation changes by at most 10% (6%) for top-quark masses chosen in the range from 20 GeV to $M_Z/2$ and $-0.9<\cos\chi<0.9$ ($-0.5<\cos\chi<0.5$).

I. INTRODUCTION

Measurement of normalized energy-energy correlations (EEC's) is one of the promising possibilities for testing QCD.[1] In fact, comparison of the QCD prediction with experimental data shows a reasonable success of QCD.[2] However, fragmentation corrections to the pure perturbative result are still large and are necessary to fit the data. It is thus a natural suggestion to go to higher energies and in particular to the Z^0 region, where the hadronic e^-e^+ annihilation cross section is large.[3,4] EEC's for these high energies have already[3,4] been calculated; also the electromagnetic corrections have been estimated.[5]

All these calculations have been carried out assuming zero quark masses, i.e., energies much higher than any quark-mass thresholds. Close to the thresholds quark-mass effects are expected to be large. With present information on the top-quark mass it is clear that the Z^0-region EEC will be affected (unless the top-quark mass is larger than half of the Z^0 mass). To estimate the effect we calculate in this paper the QCD predictions for EEC's with massive quarks. The calculation is easily done for arbitrary initial-state polarizations.

In the zero-quark-mass case the normalized, angle-integrated EEC turned out to be independent of initial-state polarizations and weak-interaction parameters (i.e., Z^0 mass and width as well as coupling constants).[4,6] Naturally this simple result will be modified in the massive-quark case. The normalized, angle-integrated EEC does depend on initial-state polarizations and weak-interaction parameters. However, these dependences turn out to be rather weak. Therefore, even close to a loosely defined quark-mass threshold the normalized angle-integrated EEC (or the asymmetry) is a useful quantity to test QCD.

The organization of the paper is as follows. In Sec. II we derive the EEC cross section as a function of the structure functions. Section III is devoted to calculating the EEC structure functions. Section IV contains a discussion of the result and numerical predictions. Some formulas are collected in the Appendix. With the help of the formulas in Sec. II and the Appendix, it is possible to calculate completely the EEC cross sections by simple numerical integrations.

II. THE ENERGY-ENERGY-CORRELATION CROSS SECTION FOR NONVANISHING QUARK MASSES

The calculation of EEC in the massive-quark case goes parallel to the zero-mass calculations. We shall follow the line of reasoning and notations of Ref. 4.

First we recall the definition of the EEC cross section.[1] Assume that a large number N of hadronic events in e^-e^+ annihilation is observed. The individual events are labeled with $A=1,\ldots,N$. In each event one measures the energies $dE_A, dE_{A'}$ carried by the hadrons into the solid angles $d\Omega=d\cos\theta\, d\phi$, $d\Omega'=d\cos\theta' d\phi'$ that lie in the directions $\hat{r}$ and $\hat{r}'$ relative to the collision point.

The normalized EEC cross section is given by

$$\frac{1}{\sigma_{\text{tot}}}\frac{d^2\Sigma}{d\Omega\, d\Omega'}=\frac{1}{N}\sum_{A=1}^{N}\left[\frac{dE_A}{W\,d\Omega}\right]\left[\frac{dE_A'}{W\,d\Omega'}\right], \tag{1}$$

where W is the total center-of-mass energy and σ_{tot} is the total hadronic cross section. The angle between $\hat{r}$ and $\hat{r}'$ is denoted by χ.

To lowest order in the electroweak interaction, the EEC is calculated by an energy-weighted phase-space integral of a squared amplitude $|T|^2$, which is given as

$$|T|^2 \propto \sum_f \left| \langle f_+ | J_{\gamma,\mu} | 0\rangle \frac{1}{W^2}\langle 0 | j_\gamma^\mu | e^-e^+\rangle + \langle f_+ | J_{\text{weak},\mu} | 0\rangle \frac{1}{W^2-M_Z^2+iM_Z\Gamma_Z}\langle 0 | j_{\text{weak}}^\mu | e^-e^+\rangle \right|^2, \tag{2}$$

where $j^\mu_{\gamma\,(\text{weak})}$ ($J^\mu_{\gamma\,(\text{weak})}$) is the lepton (hadron) electromagnetic (weak) current and f is an arbitrary outgoing hadronic final state. We rewrite this as

$$|T|^2 \propto \sum_f | a_1 v^\mu \langle f_+ | V_\mu | 0\rangle + a_2 v^\mu \langle f_+ | A_\mu | 0\rangle + a_3 a^\mu \langle f_+ | V_\mu | 0\rangle + a_4 a^\mu \langle f_+ | A_\mu | 0\rangle |^2 , \tag{3}$$

where v^μ (a^μ) is the matrix element of the vector (axial-vector) leptonic current and V_μ (A_μ) is the hadronic vector (axial-vector) current. All the coupling constants as well as the γ and Z^0 propagators are included in $a_1,\ldots,a_4$. The standard-model expressions for $a_1,\ldots,a_4$ can be easily written down; they are given in the Appendix.

As the final state is effectively invariant under charge conjugation,[3] we have the relation

$$\sum_f \langle 0|V^\mu|f_+\rangle\langle f_+|A^\nu|0\rangle=0 \tag{4}$$

in the massive-quark case, too. However, the contributions of $V^\mu V^{\nu *}$ and $A^\mu A^{\nu *}$ terms are no longer equal. We put

$$\begin{aligned}&\sum_f \langle 0|V^\mu|f_+\rangle\langle f_+|V^\nu|0\rangle\equiv\bar{V}^{\mu\nu} ,\\ &\sum_f \langle 0|A^\mu|f_+\rangle\langle f_+|A^\nu|0\rangle\equiv\bar{A}^{\mu\nu} .\end{aligned} \tag{5}$$

Neglecting final-state interactions, TCP invariance yields

$$\bar{V}^{\mu\nu}=\bar{V}^{\nu\mu} ,\quad \bar{A}^{\mu\nu}=\bar{A}^{\nu\mu} . \tag{6}$$

As in Ref. 4, the necessary integrations and polarization sums effect only the final-state particle variables, therefore they may be performed on the factors $\bar{V}^{\mu\nu},\bar{A}^{\mu\nu}$. The final results are denoted by $V^{\mu\nu},A^{\mu\nu}$. It is clear that both $V^{\mu\nu}$ and $A^{\mu\nu}$ are symmetric tensors depending on W (total energy), the quark masses, and the directions $\hat{r},\hat{r}'$ of the cones in which the energy is detected. Thus, the space-space parts have the same decomposition as in Ref. 1:

$$\begin{aligned}V_{ik}&=\mathscr{A}(\chi)(2\delta_{ik}-\hat{r}_i\hat{r}_k-\hat{r}'_i\hat{r}'_k)\\&\quad+\mathscr{B}(\chi)(\delta_{ik}\hat{r}\cdot\hat{r}'-\tfrac{1}{2}\hat{r}_i\hat{r}'_k-\tfrac{1}{2}\hat{r}'_i\hat{r}_k)\\&\quad+\mathscr{C}(\chi)\delta_{ik} ,\\ A_{ik}&=\overline{\mathscr{A}}(\chi)(2\delta_{ik}-\hat{r}_i\hat{r}_k-\hat{r}'_i\hat{r}'_k)\\&\quad+\overline{\mathscr{B}}(\chi)(\delta_{ik}\hat{r}\cdot\hat{r}'-\tfrac{1}{2}\hat{r}_i\hat{r}'_k-\tfrac{1}{2}\hat{r}'_i\hat{r}_k)\\&\quad+\overline{\mathscr{C}}(\chi)\delta_{ik} ,\end{aligned} \tag{7}$$

where the EEC structure functions $\mathscr{A},\ldots\overline{\mathscr{C}}$ do depend also on W. For the zero-quark-mass case, $\mathscr{A}=\overline{\mathscr{A}}$, $\mathscr{B}=\overline{\mathscr{B}}$, $\mathscr{C}=\overline{\mathscr{C}}$, and the structure functions—calculated to lowest order in perturbative QCD—are given in Ref. 1 (and reproduced in the Appendix). The nonzero-quark-mass expressions are calculated in Sec. III. The perturbative results should be reliable for $\chi\neq 0^0$ and $\chi\neq 180°$, provided fragmentation corrections are also added. (Results in a simple treatment of fragmentation are given in Ref. 1). Fragmentation corrections fall as $1/W$ with increasing energy; therefore near the Z^0 peak they are much less, than at currently available energies.

The EEC cross section is now given for arbitrary e^-e^+ polarizations as

$$\begin{aligned}\frac{d^2\Sigma}{d\Omega\, d\Omega'}=\frac{3W^2}{2^6\pi^2}\sum_f\,&[V_f^{ik}(v_iv_k^*|a_{1f}|^2+a_ia_k^*|a_{3f}|^2+v_ia_k^*a_{1f}a_{3f}^*+a_iv_k^*a_{1f}^*a_{3f})\\&+A_f^{ik}(v_iv_k^*|a_{2f}|^2+a_ia_k^*|a_{4f}|^2+v_ia_k^*a_{2f}a_{4f}^*+a_iv_k^*a_{2f}^*a_{4f})] ,\end{aligned} \tag{8}$$

where the sum goes over the quark flavors. The leptonic polarization tensors $v_iv_k^*,\ldots$ have been calculated,[3,4] the symmetric parts [only these enter in (8)] are reproduced in the Appendix. Only the space-space components of these tensors are nonvanishing.

It is reasonable to normalize to the total hadronic cross section given by

$$\begin{aligned}\sigma_{\rm tot}=\frac{W^2}{4\pi}\sum_f\,&\{(1-s_L\underline{s}_L)[(|a_{1f}|^2+|a_{3f}|^2)(1+2\mu_f^2)+(|a_{2f}|^2+|a_{4f}|^2)(1-4\mu_f^2)]\\&+2(\underline{s}_L-s_L){\rm Re}[a_{3f}a_{1f}^*(1+2\mu_f^2)+a_{4f}a_{2f}^*(1-4\mu_f^2)]\}(1-4\mu_f^2)^{1/2} ,\quad \mu_f=\frac{m_f}{W} ,\end{aligned} \tag{9}$$

where s_L ($\underline{s}_L$) is the longitudinal component of the polarization vector of e^- (e^+).

The form of Eq. (8) is rather complicated. To obtain simpler formulas we integrate over some of the angles $(\theta,\phi,\theta',\phi')$ modifying only the V^{ik},A^{ik} factors. For arbitrary initial polarizations we get

$$\begin{aligned}\frac{d^2\Sigma}{d\cos\chi\, d\cos\theta}=\frac{3W^2}{32}\sum_f\,&(\{\mathscr{A}_f[6-\sin^2\theta(1+\cos^2\chi)+2\cos^2\theta\cos^2\chi]+\mathscr{B}_f\cos\chi(4-2\sin^2\theta)+4\mathscr{C}_f\}\\&\times[(1-s_L\underline{s}_L)(|a_{1f}|^2+|a_{3f}|^2)+2(\underline{s}_L-s_L)(a_{3f}a_{1f}^*+a_{3f}^*a_{1f})]\\&+\{\overline{\mathscr{A}}_f[6-\sin^2\theta(1+\cos^2\chi)+2\cos^2\theta\cos^2\chi]+\overline{\mathscr{B}}_f\cos\chi(4-2\sin^2\theta)+4\overline{\mathscr{C}}_f\}\\&\times[(1-s_L\underline{s}_L)(|a_{2f}|^2+|a_{4f}|^2)+2(\underline{s}_L-s_L)(a_{4f}a_{2f}^*+a_{4f}^*a_{2f})]) ,\end{aligned} \tag{10}$$

where θ is the angle between $\hat{r}$ and the e^- momentum and

$$\frac{d\Sigma}{\alpha\cos\chi}=\frac{W^2}{4}\sum_f\{(4\mathscr{A}_f+2\cos\chi\,\mathscr{B}_f+3\mathscr{C}_f)[(1-s_L\underline{s}_L)(|a_{1f}|^2+|a_{3f}|^2)+2(\underline{s}_L-s_L)(a_{3f}a_{1f}^*+a_{3f}^*a_{1f})]$$
$$+(4\overline{\mathscr{A}}_f+2\cos\chi\,\overline{\mathscr{B}}_f+3\overline{\mathscr{C}}_f)[(1-s_L\underline{s}_L)(|a_{2f}|^2+|a_{4f}|^2)+2(\underline{s}_L-s_L)(a_{4f}a_{2f}^*+a_{4f}^*a_{2f})]\}. \quad (11)$$

The transverse components of polarization vectors drop out from Eqs. (9), (10), and (11).

While in the zero-quark-mass case

$$\frac{1}{\sigma_{\text{tot}}}\frac{\alpha^3\Sigma}{d\cos\chi\,d\cos\theta\,d\phi}\ ,\quad \frac{1}{\sigma_{\text{tot}}}\frac{d^2\Sigma}{d\cos\chi\,d\cos\theta}\ ,\ \text{and}\ \frac{1}{\sigma_{\text{tot}}}\frac{d\Sigma}{d\cos\chi}$$

were independent of initial-state polarizations and weak-interaction parameters,[4] it is clear from Eqs. (9), (10) and (11) that these dependences do not drop out in the present case. (Obviously, taking $\mathscr{A}_f=\overline{\mathscr{A}}_f=\mathscr{A}$, etc., we get back the zero-quark-mass results.) The above formulas allow us to predict completely these dependences. In practice, it turns out that for the normalized, angle-integrated EEC $[(1/\sigma_{\text{tot}})d\Sigma/d\cos\chi]$ quark-mass effects are not very large.

III. CALCULATION OF THE EEC STRUCTURE FUNCTIONS

In this section we summarize the calculation of V_{ik},A_{ik}. Since we are interested in angles $\chi\neq 0^0$, $\chi\neq 180°$ only the graphs of Fig. 1 are relevant. For γ exchange these graphs have been calculated in[7] (for the unpolarized-initial-state case only). The traces to be calculated are

$$\begin{aligned}\overline{V}^{ik}\propto \mathrm{Tr}\Bigg\{&(p\cdot\gamma+\mu)\left[\gamma^\alpha\frac{(p+k)\cdot\gamma+\mu}{2p\cdot k}\gamma^i-\gamma^i\frac{(\overline{p}+k)\cdot\gamma-\mu}{2\overline{p}\cdot k}\gamma^\alpha\right]\\&\times(\overline{p}\cdot\gamma-\mu)\left[\gamma_\alpha\frac{(\overline{p}+k)\cdot\gamma-\mu}{2\overline{p}\cdot k}\gamma^k-\gamma^k\frac{(p+k)\cdot\gamma+\mu}{2p\cdot k}\gamma_\alpha\right]\Bigg\}\ ,\\ \overline{A}^{ik}\propto \mathrm{Tr}\Bigg\{&(p\cdot\gamma+\mu)\left[\gamma^\alpha\frac{(p+k)\cdot\gamma+\mu}{2p\cdot k}\gamma^i\gamma_5-\gamma^i\gamma_5\frac{(\overline{p}+k)\cdot\gamma-\mu}{2\overline{p}\cdot k}\gamma^\alpha\right]\\&\times(\overline{p}\cdot\gamma-\mu)\left[\gamma_5\gamma^k\frac{(p+k)\cdot\gamma+\mu}{2p\cdot k}\gamma_\alpha-\gamma_\alpha\frac{(\overline{p}+k)\cdot\gamma-\mu}{2\overline{p}\cdot k}\gamma_5\gamma^k\right]\Bigg\}\ .\end{aligned} \quad (12)$$

To calculate the EEC, we have to integrate over the energy-weighted phase space, i.e.,

$$V^{ik}=\int p^2dp\,\overline{p}^2d\overline{p}\frac{d^3k}{k}\delta(1-E-\overline{E}-k)\delta^3(\vec{p}+\vec{\overline{p}}+\vec{k})\overline{V}^{ik}+2\int p^2dp\,k^2dk\,\frac{d^3\overline{p}}{\overline{E}}\,\delta(1-E-\overline{E}-k)\delta^3(\vec{p}+\vec{\overline{p}}+\vec{k})\overline{V}^{ik}\ , \quad (13)$$

and similarly for A^{ik}.[8] The first integral represents the contribution, when the energies of the q and $\overline{q}$ are measured in $d\Omega$ and $d\Omega'$, respectively, and the gluon is integrated over. (It is understood that the opposite contribution, i.e., $\overline{q}$ in $d\Omega$ and q in $d\Omega'$, is also added.) The second integral represents the contribution, when the qg energies are measured (again the opposite contributions, i.e., gq, are added). The factor 2 takes into account the $\overline{q}g$ $(g\overline{q})$ contributions.

After taking into account energy-momentum conservation, $V^{ik}(A^{ik})$ is given as a sum of two one-dimensional integrals. Since we cannot evaluate these integrals analytically and are interested in the EEC structure functions, we multiply by appropriate projection operators[1] below the integration sign. We use the projectors

$$P_{1ik}=\frac{(r+r')_i(r+r')_k}{2(1+r\cdot r')}\ ,\quad P_{2ik}=\frac{(r-r')_i(r-r')_k}{2(1-r\cdot r')}\ ,\quad P_{3ik}=\delta_{ik}-P_{1ik}-P_{2ik}\ . \quad (14)$$

These project out the functions A_1,A_2,A_3 $(\overline{A}_1,\overline{A}_2,\overline{A}_3)$ which are easily connected to our structure functions:[1]

$$\begin{aligned}\mathscr{A}&=[-\tfrac{1}{2}A_1(1-\cos\chi)-\tfrac{1}{2}A_2(1+\cos\chi)+A_3]\frac{1}{\sin^2\chi}\ ,\\ \mathscr{B}&=[-A_1(1-\cos\chi)+A_2(1+\cos\chi)-A_3 2\cos\chi]\frac{1}{\sin^2\chi}\ ,\\ \mathscr{C}&=A_1+A_2-A_3\ ,\end{aligned} \quad (15)$$

and similarly for $\overline{\mathscr{A}}$, $\overline{\mathscr{B}}$, and $\overline{\mathscr{C}}$.

The limits of integration in Eq. (13) are obtained from kinematics. The case of the first integral ($q\overline{q}$ contribution) is somewhat tricky. If we choose to eliminate the $d^3k\,d\overline{p}$ integration we are left with, e.g.,

$$\int dp\, p^2\bar{p}^2 \frac{\bar{E}}{|\bar{p}(1-E)+p\bar{E}\cos\mathcal{X}|} P_1^{ik}\bar{V}_{ik}\ , \tag{16}$$

where in the integrand we have to put

$$k=(p^2+\bar{p}^2+2p\bar{p}\cos\mathcal{X})^{1/2}\ ,\quad \bar{E}=(\bar{p}^2+\mu^2)^{1/2}\ ,$$
$$\bar{p}_{\pm}=\frac{p\cos\mathcal{X}(1-2E+2\mu^2)\pm(1-E)[(1-2E)^2-4\mu^2p^2\sin^2\mathcal{X}]^{1/2}}{2[p^2\cos^2\mathcal{X}-(1-E)^2]}\ . \tag{17}$$

For $\cos\mathcal{X}>0$ we have to choose $\bar{p}_-$ and for the integration range we have

$$p\in\left[0,\frac{1-2\mu}{2(1-\mu)}\right]\ . \tag{18}$$

For $\cos\mathcal{X}<0$ both $\bar{p}_+$ and $\bar{p}_-$ yield acceptable kinematical configurations for appropriate values of p. Choosing $\bar{p}_-$ the range of p integration is

$$p\in(0,p_1)\ , \tag{19}$$

where $p_1=(E_1{}^2-\mu^2)^{1/2}$,

$$E_1=\frac{1-\mu\sin\mathcal{X}(1-4\mu^2+4\mu^4\sin^2\mathcal{X})^{1/2}}{2(1-\mu^2\sin^2\mathcal{X})}\ . \tag{20}$$

Choosing $\bar{p}_+$ the range of p integration is

$$p\in\left[\frac{1-2\mu}{2(1-\mu)},p_1\right]\ . \tag{21}$$

Obviously, we have to add these two integrals. To illustrate the situation $\bar{p}_{\pm}(p)$ is plotted on Fig. 2 for $\cos\mathcal{X}<0$.

In practice it is not advisable to calculate the integral in this way. Namely, the "Jacobian" $\propto[\bar{p}(1-E)+p\bar{E}\cos\mathcal{X}]^{-1}$ is singular at p_1 (for $\cos\mathcal{X}<0$). Although this fact does not mean that the integral is infinite, from the point of view of numerical integration it is better to avoid the singular point. We utilize the fact that $P_1^{ik}\bar{V}_{ik}$ (and all the other functions) are symmetric with respect to the exchange of q and $\bar{q}$ variables, therefore, we calculate

$$2\int_0^{p_2} dp\, p^2\bar{p}^2\frac{\bar{E}}{\bar{p}(1-E)+p\bar{E}\cos\mathcal{X}}P_1^{ik}\bar{V}_{ik}\ , \tag{22}$$

i.e., "half" of the integral, multiplied by 2. The limit p_2 is determined by the condition

$$\bar{p}_-(p_2)=p_2\ . \tag{23}$$

The second-integral does not offer any complications. After carrying out the $d^3\bar{p}\,dk$ integrals, the range of the p integral is

$$p\in\left[0,\left[\frac{1-4\mu^2}{4}\right]^{1/2}\right]\ . \tag{24}$$

The final results of all these calculations are given in the Appendix. Using the formulas given there it is easy to

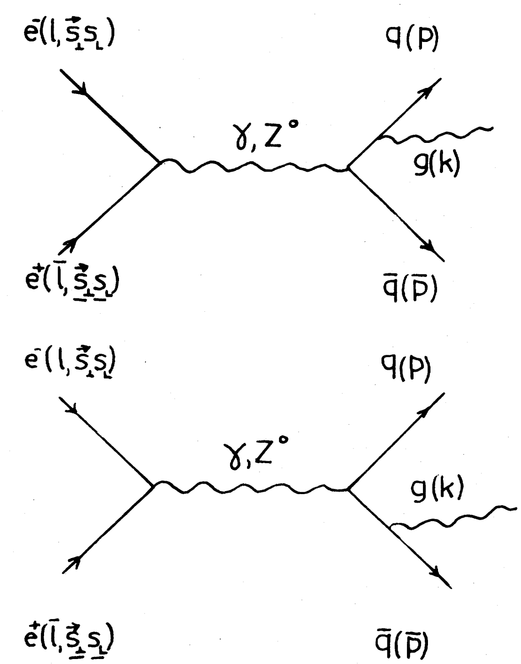

FIG. 1. Lowest-order graphs for EEC cross section at $\mathcal{X}\neq 0°$, $\mathcal{X}\neq 180°$.

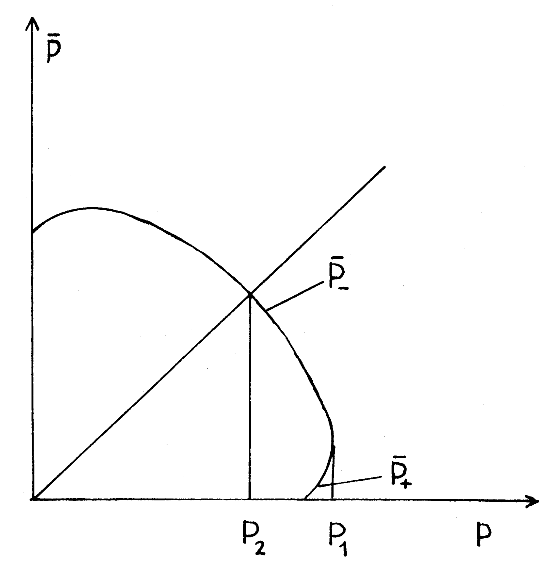

FIG. 2. The physical region of the function $\bar{p}\,(p)$ for $\cos\mathcal{X}<0$. Note that the figure is drawn disproportionately in order to emphasize that the function is double valued.

determine $\mathscr{A},\ldots,\overline{\mathscr{C}}$ for arbitrary quark masses by carrying out a few one-dimensional numerical integrals.

IV. DISCUSSION

In this section we discuss the numerical changes caused by nonzero quark masses in the EEC cross section. We calculate for the unpolarized-initial-state case and integrate over all angles except for χ, i.e., we use Eqs. (9) and (11) with $s_L=\underline{s}_L=0$.

Figure 3 shows the contribution of one massive quark divided by the zero-mass contribution for the vector-vector and axial-vector—axial-vector terms separately (i.e., we plot

$$\frac{(4\mathscr{A}+2\cos\chi\mathscr{B}+3\mathscr{C})(\mu\neq0)}{(4\mathscr{A}+2\cos\chi\mathscr{B}+3\mathscr{C})(\mu=0)}$$

and

$$\frac{(4\overline{\mathscr{A}}+2\cos\chi\overline{\mathscr{B}}+3\overline{\mathscr{C}})(\mu\neq0)}{(4\overline{\mathscr{A}}+2\cos\chi\overline{\mathscr{B}}+3\overline{\mathscr{C}})(\mu=0)} .$$

Note that for $\mu=0$, $\mathscr{A}=\overline{\mathscr{A}}$, etc.). It is clear that the effect is large, especially for the axial-vector—axial-vector terms. However, we have to add the contributions of several quarks, most of which are light. Furthermore, in the normalized quantity a very heavy quark does not contribute much. When the quark mass is $W/2$ the heavy quark does not contribute at all. In Figs. 4 and 5 we have plotted $(1/\sigma_{\rm tot})d\Sigma/d\cos\chi$ at $W=77$ GeV and $W=M_Z$. The weak interaction parameters are taken from the standard model with $\sin^2\theta_W=0.231$. We have put α_s equal to 0.13. Also the width Γ_z of the Z^0 is calculated for nonzero t-quark mass m_t. All the quark masses are taken to be zero except for the t-quark mass. For m_t we have assumed several values in the range (20 GeV, $M_Z/2$). The deviation of $(1/\sigma_{\rm tot})d\Sigma/d\cos\chi$ from the $m_t=0$ value is rather small. Therefore we have plotted

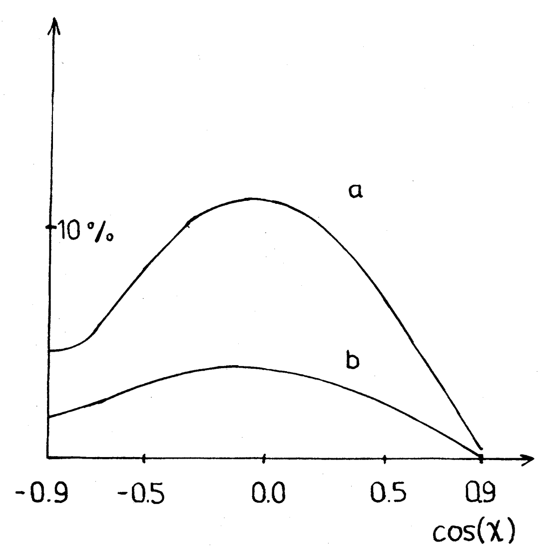

FIG. 3. Ratios of the massive-quark and zero-quark-mass contributions to $d\Sigma/d\cos\chi$ for a single flavor; (a) shows the vector-vector contributions, (b) the axial-vector—axial-vector contributions. The quark mass is $\frac{35}{90}$ (in units of W).

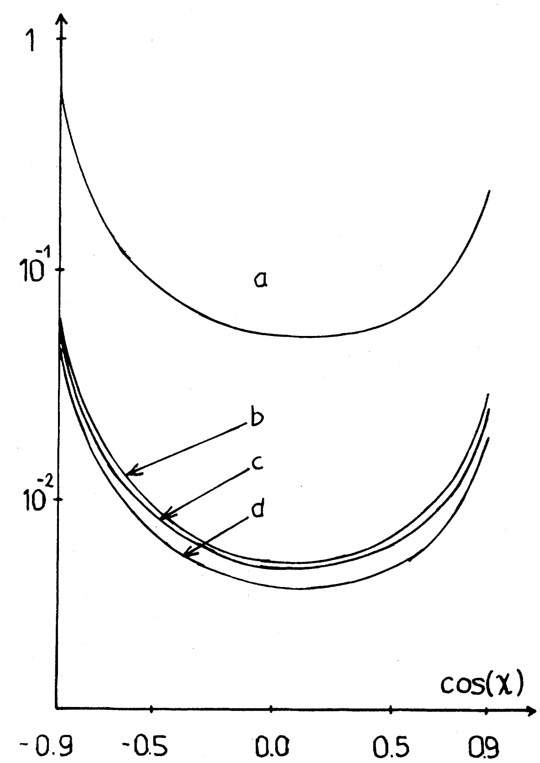

FIG. 4. (a) $(1/\sigma_{\rm tot})d\Sigma/d\cos\chi$ for zero-quark masses at $W=77$ GeV. (b)—(d) show

$$\frac{1}{\sigma_{\rm tot}}\frac{d\Sigma}{d\cos\chi}\bigg|_{m_t=0}-\frac{1}{\sigma_{\rm tot}}\frac{d\Sigma}{d\cos\chi}\bigg|_{m_t\neq0}$$

for top-quark masses $m_t=30$, 35 and 40 GeV, at $W=77$ GeV.

$$\frac{1}{\sigma_{\rm tot}}\frac{d\Sigma}{d\cos\chi}(m_t=0)-\frac{1}{\sigma_{\rm tot}}\frac{d\Sigma}{d\cos\chi}(m_t\neq0)$$

in Figs. 4 and 5 on a logarithmic scale.

There are two effects determining the value of $1/\sigma_{\rm tot}d\Sigma/d\cos\chi$ in Fig. 4. Increasing m_t $\sigma_{\rm tot}$ decreases (the change is $\approx15\%$) and also the value of $d\Sigma/d\cos\chi$ decreases. The case of Fig. 5, i.e., $W=M_Z$ is somewhat exceptional. Namely, roughly $\sigma_{\rm tot}\propto1/\Gamma_Z{}^2$, i.e., when m_t increases, $\sigma_{\rm tot}$ increases (the change is $\approx13\%$). However, $d\Sigma/d\cos\chi$ is also roughly proportional to $1/\Gamma_Z{}^2$, therefore the effect of the variation of the Z^0 width is partially compensated. As a result the effect of nonzero m_t is even smaller at $W=M_Z$ than at somewhat lower energies.

Quark-mass effects on the asymmetry, defined[1] as

$$\frac{1}{\sigma_{\rm tot}}\left[\frac{d\Sigma}{d\cos\chi}(180^\circ-\chi)-\frac{d\Sigma}{d\cos\chi}(\chi)\right],$$

are even smaller than those for normalized EEC cross sections. The results for $W=M_Z$ and several m_t values are given in Table I.

Figure 6 shows our curve for $W=30$ GeV, $m_c=1.6$ GeV, and $m_b=5$ GeV. For this low energy the Z^0 contribution is negligible. Therefore, our result here agrees with Ref. 9 (where quark-mass effects on EEC without Z^0 exchange have been calculated). It is clear that the

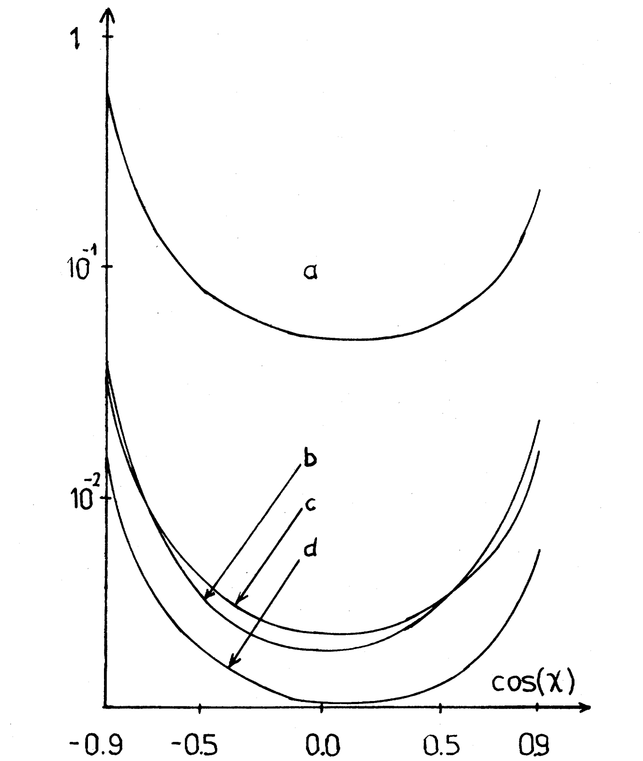

FIG. 5. (a) $(1/\sigma_{\rm tot})d\Sigma/d\cos\chi$ for zero quark masses at $W=M_Z$. (b)—(d) show

$$\frac{1}{\sigma_{\rm tot}}\frac{d\Sigma}{d\cos\chi}\bigg|_{m_t=0}-\frac{1}{\sigma_{\rm tot}}\frac{d\Sigma}{d\cos\chi}\bigg|_{m_t\neq 0}$$

for top-quark masses $m_t=20$, 30, and 40 GeV, at $W=M_Z$.

zero-mass-QCD prediction is not much changed. However, it is possible to enhance quark-mass effects if EEC's are measured in flavor-tagged events.[10] Figure 6 shows the normalized EEC for the sample of flavor-tagged events of Ref. 10, i.e., events containing 44% $b\bar{b}$, 41% $c\bar{c}$ decay.

In summary, we have calculated EEC with nonzero quark masses.

Large quark-mass effects may be looked for in unnormalized, fully differential EEC, with polarized initial

TABLE I. Normalized asymmetry at $W=M_Z$ for several top-quark-mass values. $m_t=0$ is given for comparison.

$\cos\chi$ \ m_t	0	20 GeV	30 GeV	40 GeV
0.9	0.3557	0.3345	0.3344	0.3461
0.8	0.1203	0.1149	0.1135	0.1171
0.7	0.0611	0.0590	0.0579	0.0595
0.6	0.0365	0.0356	0.0347	0.0355
0.5	0.0236	0.0231	0.0225	0.0229
0.4	0.0157	0.0155	0.0151	0.0153
0.3	0.0103	0.0102	0.0099	0.0101
0.2	0.0063	0.0063	0.0061	0.0062
0.1	0.0030	0.0030	0.0029	0.0029
0.0	0.0	0.0	0.0	0.0

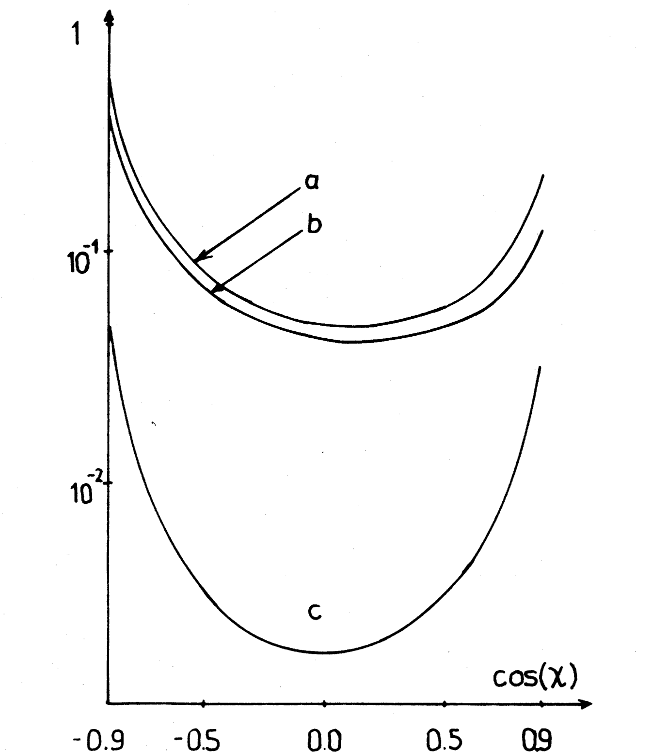

FIG. 6. (a) $(1/\sigma_{\rm tot})d\Sigma/d\cos\chi$ for zero-quark masses at $W=30$ GeV. (b) $(1/\sigma_{\rm tot})d\Sigma/d\cos\chi$ for the flavor-tagged events of Ref. 10 for $m_c=1.6$ GeV, $m_b=5$ GeV at $W=30$ GeV. (c)

$$\frac{1}{\sigma_{\rm tot}}\frac{d\Sigma}{d\cos\chi}\bigg|_{m_c=m_b=0}-\frac{1}{\sigma_{\rm tot}}\frac{d\Sigma}{d\cos\chi}\bigg|_{m_c,m_b\neq 0}$$

for $m_c=1.6$ GeV, $m_b=5$ GeV at $W=30$ GeV.

state. The QCD predictions may be obtained with the help of our formulas in Sec. II and the Appendix. While the simple properties of EEC cross sections with zero-quark masses—i.e., independence of

$$\frac{1}{\sigma_{\rm tot}}\frac{d^3\Sigma}{d\cos\chi\,d\cos\theta d\phi}\,,\quad \frac{1}{\sigma_{\rm tot}}\frac{d^2\Sigma}{d\cos\chi\,d\cos\theta}\,,$$
$$\frac{1}{\sigma_{\rm tot}}\frac{d\Sigma}{d\cos\chi}$$

on initial-state polarizations and weak-interaction parameters[4]—are invalidated, the effects of nonzero quark masses on $(1/\sigma_{\rm tot})d\Sigma/d\cos\chi$ are very small. The total cross section (and also unnormalized EEC) is much more sensitive to quark-mass effects than the normalized EEC cross sections. This again underlines the importance of experimental determinations of normalized EEC cross sections. Quark-mass effects on the asymmetry are even smaller than those for normalized EEC cross sections. The Z^0 peak region emerges as a particularly good possibility to test QCD via measurement of $(1/\sigma_{\rm tot})d\Sigma/d\cos\chi$ and the asymmetry. In this region the hadronic cross section is large, fragmentation corrections are smaller by a factor $\frac{1}{3}$ than those at currently accessible energies, electromagnetic corrections are very small,[5] and— as shown is this paper—t-quark-mass effects are small, even if this region is close to the t-quark-mass threshold.

Note added. In a recent paper[11] Cho, Han, and Kim have independently calculated EEC taking into account both Z^0-exchange and quark-mass effects. We have compared the results and found complete agreement. In comparing the numerical results one should keep in mind that Ref. 11 normalizes to the pointlike (1γ) total cross section $\sigma_0=4\pi\alpha^2/(3W^2)$, while we normalize to the physical total cross section $\sigma_{\rm tot}$. The advantages of our normalization are discussed in Ref. 4 and in the text. Since $\sigma_{\rm tot}$ also depends on quark masses, our normalized EEC's show much less quark-mass dependences. We emphasize, that the formulas given in our appendix are better suited for numerical integration than those of Ref. 11, in particular we have also included a discussion of the integration region.

ACKNOWLEDGMENTS

I am grateful to G. Pócsik for encouragement and reading the manuscript and thank E. Lendvai for helpful discussions.

APPENDIX

The propagator factors of Eqs. (3) and (8)—(11) are given here for flavor f:[4]

$$
\begin{aligned}
a_{1f}&=\frac{e^2}{W^2}Q_f+\frac{g_V G_{Vf}}{W^2-M_Z{}^2+iM_Z\Gamma_Z}\ ,\\
a_{2f}&=\frac{g_V G_{Af}}{W^2-M_Z{}^2+iM_Z\Gamma_Z}\ ,\\
a_{3f}&=\frac{g_A G_{Vf}}{W^2-M_Z{}^2+iM_Z\Gamma_Z}\ ,\\
a_{4f}&=\frac{g_A G_{Af}}{W^2-M_Z{}^2+iM_Z\Gamma_Z}\ ,
\end{aligned}
\qquad \text{(A1)}
$$

where

$$g_V=(1-4\sin^2\theta_W)e/(4\sin\theta_W\cos\theta_W)\ ,$$

$$g_A=e/(4\sin\theta_W\cos\theta_W)\ ,$$

eQ_f is the charge of the quark, and for positive charge

$$G_{Vf}=g_A(1-\tfrac{8}{3}\sin^2\theta_W)\ ,$$

$$G_{Af}=g_A\ ,$$

while for negative charge

$$G_{Vf}=g_A(-1+\tfrac{4}{3}\sin^2\theta_W)\ ,$$

$$G_{Af}=-g_A\ .$$

θ_W is the Weinberg angle and M_Z and Γ_Z are the Z^0 mass and width.

The symmetric parts of the leptonic polarization tensors are given by[3,4]

$$
\begin{aligned}
v^i v^{k*}&=(\delta^{ik}-\delta^{i3}\delta^{k3})(1+\vec{s}_\perp\cdot\underline{\vec{s}}_\perp-s_L\underline{s}_L)\\
&\quad-\underline{s}^i_\perp s^k_\perp-\underline{s}^k_\perp s^i_\perp\ ,\\
a^i a^{k*}&=(\delta^{ik}-\delta^{i3}\delta^{k3})(1-\vec{s}_\perp\cdot\underline{\vec{s}}_\perp-s_L\underline{s}_L)\\
&\quad+\underline{s}^i_\perp s^k_\perp+\underline{s}^k_\perp s^i_\perp\ ,\\
v^i a^{k*}&=(\underline{s}_L-s_L)(\delta^{ik}-\delta^{i3}\delta^{k3})\\
&\quad+i(s^1_\perp\underline{s}^1_\perp-s^2_\perp\underline{s}^2_\perp)(\delta^{i1}\delta^{k2}+\delta^{i2}\delta^{k1})\ ,
\end{aligned}
\qquad \text{(A2)}
$$

where $(\vec{s}_\perp,s_L)$ $[(\underline{\vec{s}}_\perp,\underline{s}_L)]$ refer to the e^- $[e^+]$ polarization vectors, and e^- moves in the direction of the third axis, while e^+ moves opposite to it. The polarization vectors are defined as in Ref. 3.

The lowest-order QCD structure functions for zero-quark mass are given by[1]

$$
\begin{aligned}
\mathscr{A}&=\frac{\alpha_s}{12\pi^2}\frac{1}{1-\xi}\left[\frac{3-4\xi}{\xi^5}\ln(1-\xi)+\frac{3}{\xi^4}-\frac{5}{2\xi^3}-\frac{1}{\xi^2}\right],\\
\mathscr{B}&=\frac{\alpha_s}{12\pi^2}\frac{1}{1-\xi}\left[\frac{4(3-\xi)(1-\xi)}{\xi^5}\ln(1-\xi)+\frac{12}{\xi^4}-\frac{10}{\xi^3}\right],\\
\mathscr{C}&=0\ ,
\end{aligned}
\qquad \text{(A3)}
$$

α_s is the running strong coupling at energy W and $\xi=\frac{1}{2}(1-\cos\chi)$.

We summarize here our results for the structure functions $\mathscr{A},\mathscr{B},\mathscr{C}$ $(\overline{\mathscr{A}},\overline{\mathscr{B}},\overline{\mathscr{C}})$ of V_{ik} (A_{ik}). First, we decompose all of them into the $q\bar{q}$ and qg contributions, e.g.,

$$\mathscr{A}=\mathscr{A}_{q\bar{q}}+2\mathscr{A}_{qg}\ . \qquad \text{(A4)}$$

Then we write the $q\bar{q}$ and qg contributions in the form of integrals and specify later the integrands of the integrals, e.g.,

$$
\begin{aligned}
\mathscr{A}_{q\bar{q}}&=\frac{8\alpha_s}{3\pi^2}\int_0^{p_2}dp\,2p^2\bar{p}^2\frac{\bar{E}}{\bar{p}(1-E)+p\bar{E}\cos\chi}a_{q\bar{q}}\ ,\\
\mathscr{A}_{qg}&=\frac{8\alpha_s}{3\pi^2}\int_0^{p_3}dp\frac{p^2}{(1-h)^2}a_{qg}\ .
\end{aligned}
\qquad \text{(A5)}
$$

We use the following notations:[8]

α_s is the strong coupling at energy W, μ is the quark mass, $E=(p^2+\mu^2)^{1/2}$,

$$\bar{p}=\frac{p\cos\chi(1-2E+2\mu^2)-(1-E)[(1-2E)^2-4\mu^2p^2\sin^2\chi]^{1/2}}{2[p^2\cos^2\chi-(1-E)^2]}\ ,\quad \bar{E}=(\bar{p}^2+\mu^2)^{1/2}\ ,$$

$$k=\frac{1-2E}{2(1-h)}\ ,\quad h=E-p\cos\chi\ ,\quad p_2 \text{ is the root[12] of the equation } \bar{p}(p_2)=p_2\ ,\quad p_3=\left[\frac{1-4\mu^2}{4}\right]^{1/2}\ . \qquad \text{(A6)}$$

With these notations we have

$$
\begin{aligned}
a_{q\bar q}&=\frac{2(p^2+\bar p^2)}{(1-2E)(1-2\bar E)}-\frac{4\mu^2p^2}{(1-2E)^2}-\frac{4\mu^2\bar p^2}{(1-2\bar E)^2}\,,\\
b_{q\bar q}&=\frac{16\mu^2p\bar p}{(1-2E)(1-2\bar E)}\,,\\
c_{q\bar q}&=2\mu^2\left[\frac{2-8p\bar p\cos\chi}{(1-2E)(1-2\bar E)}+\frac{4p^2-1}{(1-2E)^2}+\frac{4\bar p^2-1}{(1-2\bar E)^2}\right],\\
a_{qg}&=\frac{p^2(1-2\mu^2)+k^2/2}{h}-\frac{\mu^2p^2}{1-h}-\frac{\mu^2(p^2+k^2)(1-h)}{h^2}\,,\\
b_{qg}&=2pk\left[1-\frac{2\mu^2}{h}\right]\frac{1}{h}\,,\\
c_{qg}&=\frac{\mu^2}{2h}\left[8p^2+8pk\cos\chi+2+(p^2+k^2+2pk\cos\chi)\frac{4(1-h)}{h}-\frac{1-h}{h}+\frac{(4p^2-1)h}{1-h}\right],
\end{aligned}
\tag{A7}
$$

$$
\begin{aligned}
\bar a_{q\bar q}-a_{q\bar q}&=-\frac{8\mu^2(p^2+\bar p^2)}{(1-2E)(1-2\bar E)}\,,\\
\bar b_{q\bar q}-b_{q\bar q}&=-\frac{32\mu^2p\bar p}{(1-2E)(1-2\bar E)}\,,\\
\bar c_{q\bar q}-c_{q\bar q}&=4\mu^2\left\{\frac{4(p^2+\bar p^2+2p\bar p\cos\chi)-2(E+\bar E)}{(1-2E)(1-2\bar E)}\right.\\
&\quad\left.+\frac{1}{1-2E}+\frac{1}{1-2\bar E}+2\mu^2\left[\frac{2}{(1-2E)(1-2\bar E)}+\frac{1}{(1-2E)^2}+\frac{1}{(1-2\bar E)^2}\right]\right\},\\
\bar a_{qg}-a_{qg}&=-\frac{2\mu^2k^2}{h}\,,\\
\bar b_{qg}-b_{qg}&=0\,,\\
\bar c_{qg}-c_{qg}&=\frac{2\mu^2}{h}(-1+2k+2k^2)+2\mu^4\left[\frac{1}{h}+\frac{1}{h^2}+\frac{1}{1-h}\right].
\end{aligned}
\tag{A8}
$$

The above integrals are given in a form which makes numerical integration straightforward. In particular none of the denominators are zero.

---

[1]C. L. Basham, L. S. Brown, S. D. Ellis, and S. T. Love, Phys. Rev. Lett. 41, 1585 (1978); Phys. Rev. D 19, 2018 (1979); L. S. Brown and S. D. Ellis, *ibid.* 24, 2383 (1981).

[2]Ch. Berger *et al.*, Phys. Lett. 99B, 292 (1981); H. J. Behrend *et al.*, Z. Phys. C 14, 95 (1982); D. Schlatter *et al.*, Phys. Rev. Lett. 49, 521 (1982); D. M. Ritson, in *Proceedings of the 21st International Conference on High Energy Physics, Paris, 1982*, edited by P. Petiau and M. Porneuf [J. Phys. (Paris) Colloq. 43, (1982)], p. 52; B. Adeva *et al.*, Phys. Rev. Lett. 50, 2051 (1983).

[3]L. S. Brown and S. P. Li, Phys. Rev. D 26, 570 (1982).

[4]F. Csikor, G. Pócsik, and A. Tóth, Phys. Rev. D 28, 1206 (1983).

[5]F. Csikor, G. Pócsik, and A. Tóth, Phys. Rev. D 28, 2877 (1983).

[6]Note that this result is valid for both perturbative (to arbitrary order in α_s) and nonperturbative contributions.

[7]B. L. Joffe, Phys. Lett. 78B, 227 (1978).

[8]All the momenta and energies are measured in units of W, $\mu=m/W$.

[9]A. Ali and F. Barreiro, DESY Report No. 83-070, 1983 (unpublished).

[10]D. M. Ritson (Ref. 2).

[11]K. H. Cho, S. K. Han, and J. K. Kim, Nucl. Phys. B233, 161 (1984).

[12]This equation has only a single root in the range of interest, i.e., for $\cos\chi>0$, $p\in\{0,(1-2\mu)/[2(1-\mu)]\}$; for $\cos\chi<0$, $p\in(0,p_1)$ where p_1 is defined in Eq. (20). The root may be easily obtained by numerical methods.